

# Plus end-specific depolymerase activity of Kip3, a kinesin-8 protein, explains its role in positioning the yeast mitotic spindle

Mohan L. Gupta, Jr.<sup>1</sup>, Pedro Carvalho<sup>1</sup>, David M. Roof<sup>2,3</sup> and David Pellman<sup>1,4</sup>

**The budding yeast protein Kip3p is a member of the conserved kinesin-8 family of microtubule motors, which are required for microtubule–cortical interactions, normal spindle assembly and kinetochore dynamics. Here, we demonstrate that Kip3p is both a plus end-directed motor and a plus end-specific depolymerase — a unique combination of activities not found in other kinesins. The ATPase activity of Kip3p was activated by both microtubules and unpolymerized tubulin. Furthermore, Kip3p in the ATP-bound state formed a complex with unpolymerized tubulin. Thus, motile kinesin-8s may depolymerize microtubules by a mechanism that is similar to that used by non-motile kinesin-13 proteins. Fluorescent speckle analysis established that, *in vivo*, Kip3p moved toward and accumulated on the plus ends of growing microtubules, suggesting that motor activity brings Kip3p to its site of action. Globally, and more dramatically on cortical contact, Kip3p promoted catastrophes and pausing, and inhibited microtubule growth. These findings explain the role of Kip3p in positioning the mitotic spindle in budding yeast and potentially other processes controlled by kinesin-8 family members.**

Microtubules are dynamic cytoskeletal filaments that have a central role in intracellular organization and in cell division<sup>1</sup>. Force-generating motor proteins, kinesins and dyneins, are essential for many microtubule-based processes; these motors transport cargo and organize microtubules into structures, such as the mitotic spindle<sup>2</sup>.

Over the past ten years, it has also become apparent that motor proteins, by a variety of mechanisms, have critical functions in regulating microtubule dynamics. Kinesin motors can stabilize microtubules by transporting microtubule-binding proteins to the tips of microtubules<sup>3,4</sup>. Kinesins can also directly regulate microtubule dynamics without using directed motility: Kinesin-13 proteins lack motility but are microtubule depolymerases that catalytically remove tubulin from the ends of microtubules<sup>5</sup>. MCAK (and related kinesin-13 proteins) is thought to promote microtubule disassembly through a mechanism that involves binding

to the terminal tubulin subunit(s). Kinesin-14 proteins (for example, Kar3p) are minus end-directed motors that also promote microtubule disassembly through an unknown mechanism that seems to be distinct from that of kinesin-13 proteins<sup>6,7</sup>.

It is postulated that the conserved kinesin-8-family proteins are important for regulating microtubule dynamics in diverse organisms. Genetic experiments have shown that loss of kinesin-8 proteins usually results in long microtubules<sup>8–12</sup>. Kinesin-8 proteins are important for microtubule–cortical interactions, mitochondrial distribution, kinetochore dynamics, spindle morphogenesis and chromosome segregation<sup>8–19</sup>. Although the mechanisms by which these proteins control microtubule dynamics and/or other aspects of microtubule function is not understood, some kinesin-8 proteins seem to be plus end-directed motors<sup>16,17</sup>. Additionally, the motor domain of kinesin-8 proteins is least evolutionarily divergent from the kinesin-13 depolymerases, leading to the hypothesis that kinesin-8 proteins may also be depolymerases<sup>20,21</sup>; however, recent structural studies imply that the depolymerase activity of kinesin-13 proteins may not be compatible with microtubule motility<sup>22,23</sup>.

Here, we show that the budding yeast kinesin-8, Kip3p, is both a plus end-directed motor and a plus end-specific depolymerase. Although Kip3p lacks the structural features that are proposed to be important for depolymerization by kinesin-13 proteins, and exclusively depolymerizes plus ends, it shares distinct biochemical properties with kinesin-13 family members that are thought to be central to the kinesin-13 depolymerization mechanism. Within cells, Kip3p is observed as speckles that travel toward, and accumulate at, the plus ends of growing microtubules. In addition to a role in regulating kinetochore dynamics<sup>18</sup> and spindle stability<sup>24,25</sup>, Kip3p is required for the initial step in aligning the position of the mitotic spindle with the plane of cell division<sup>8–10</sup>. Our genetic and live-cell imaging experiments reveal why Kip3p is required for this process: Kip3p is necessary to regulate the length of microtubules attached to the cell cortex. Thus, Kip3p is a unique kinesin with biochemical properties that explain its diverse cellular roles.

<sup>1</sup>Department of Pediatric Oncology, Dana-Farber Cancer Institute and Division of Hematology/Oncology, Children's Hospital Boston and Harvard Medical School, Boston, MA 02115, USA. <sup>2</sup>Program in Cell and Molecular Biology, Department of Animal Biology, University of Pennsylvania, 3800 Spruce Street, Philadelphia, PA 19104–6046, USA. <sup>3</sup>Current address: Cytokinetics, Inc. 280 East Grand Avenue South San Francisco, CA 94080, USA.

<sup>4</sup>Correspondence should be addressed to D.P. (e-mail: david\_pellman@dfci.harvard.edu)

Received 8 May 2006; accepted 27 July 2006; published online 13 August 2006; DOI: 10.1038/ncb1457

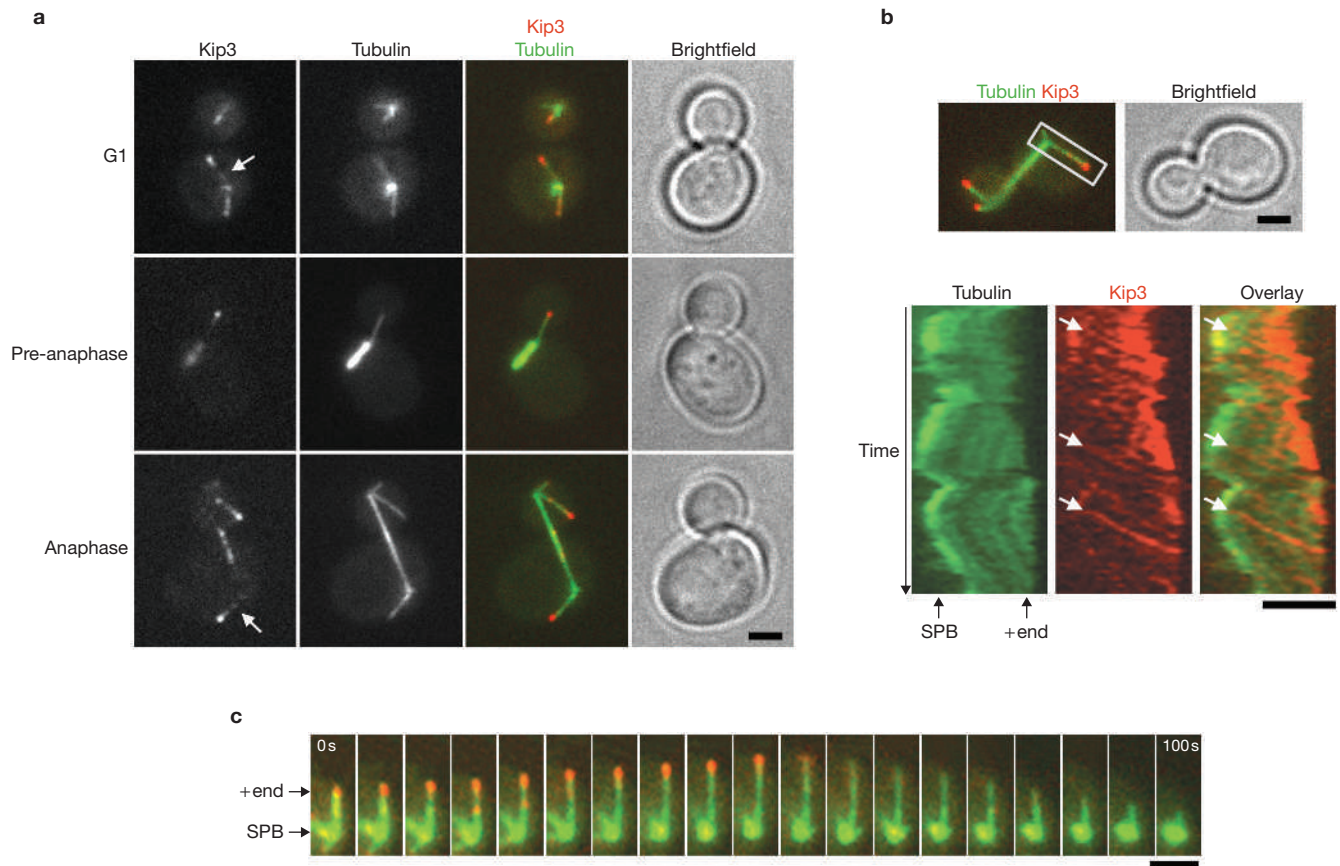


**Figure 1** Kip3p is a motor protein exhibiting plus-end tracking behaviour. (a) Kip3p is visualized as dim speckles along microtubules (arrows) and as bright spots at the plus ends of microtubules. Representative cells at different cell cycle stages labelled with CFP-Tub1p (green in the merged image) and Kip3p-3YFP (red in the merged image). (b) FSM suggests that Kip3p is a plus end-directed motor. Dual-colour single focal plane imaging of the boxed microtubule (top) is displayed as kymographs (bottom). Kip3p-3YFP speckles move continuously to the plus end at

speeds that exceed, by a factor of three, the rate of microtubule growth (arrows). The CFP-Tubulin fluorescence intensity demonstrates that the Kip3p-3YFP streaks are not associated with the growing plus end of a shorter microtubule bundled with the longer one. The entire kymograph *y*-axis represents 240 s. (c) Kip3p accumulates at the plus ends of growing, but not shortening microtubules. The images depict a single focal plane time-lapse of the same microtubule at 5.5 s intervals. The scale bars represent 2  $\mu$ m.

## RESULTS

### Kip3p moves along microtubules and behaves like a plus end tracking protein (+TIP)

Kip3p localization and dynamics were characterized *in vivo*. In contrast with previous studies of overexpressed Kip3p<sup>9,10</sup>, a functional Kip3p-3YFP fusion protein expressed under the endogenous promoter strongly and specifically localized to the plus ends of cytoplasmic microtubules throughout the cell cycle (Fig. 1a and see Supplementary Information, Fig. S1). In addition to the heavy plus-end localization, Kip3p-3YFP was also visualized as dimmer, discontinuous speckles along the length of cytoplasmic microtubules. Consistent with previous studies<sup>9,18</sup>, in mitotic cells Kip3p-3YFP also localized in a bi-lobed manner on short metaphase-like preanaphase spindles and was concentrated at the spindle midzone during anaphase (Fig. 1a).

Fluorescent speckle microscopy (FSM)<sup>26</sup> was used to evaluate whether Kip3p moved to the microtubule plus end by directed motility. Kymographs of Kip3p-3YFP fluorescence demonstrated directional movement of Kip3p from the region of the spindle pole body (SPB, the yeast counterpart of the centrosome) to the plus end of the microtubule (Fig. 1b and see Supplementary Information, Movie 1). Kip3p-3YFP speckles moved with near constant velocities that exceeded the rate of

microtubule elongation by  $\sim 3.5$ -fold (mean = 4.43  $\mu$ m min<sup>-1</sup>; s.d  $\pm 1.1$ ; range = 3.0–7.8; *n* = 41 speckles from 15 microtubules). Parallel kymographic analysis of CFP- $\alpha$ -tubulin (CFP-Tub1p) demonstrated that the Kip3p speckles did travel along the microtubule lattice and were not, for example, associated with the plus end of a shorter microtubule that was growing alongside the longer one (Fig. 1b). Plus end-directed movement of Kip3p was observed during all stages of the cell cycle. Thus, consistent with previous studies on *Aspergillus* KipB<sup>17</sup>, these imaging studies demonstrated that Kip3p translocates toward microtubule plus ends *in vivo*.

When Kip3p-3YFP fluorescence was measured, we found that although 28% of microtubules had an intense concentration of Kip3p at the plus end (>eightfold above cytosolic background; *n* = 251), another 54% displayed intermediate intensity (2–8-fold increase) and the final 18% had little, if any, Kip3p signal at the plus end. This suggested that Kip3p accumulates on a specific subset of microtubules. Using time-lapse microscopy, Kip3p was observed to be strongly concentrated at the tips of growing microtubules and was reduced or absent from depolymerizing plus ends (Fig. 1c and see Supplementary Information, Movie 2). Thus, Kip3p displays common features with microtubule +TIPs<sup>27</sup>. These findings, together with the observations that inhibition of kinesin-8 motors in widely different cell types results in long

**Table 1** Microtubule behaviour during *in vitro* gliding assays

	Kip3		Kinesin	
	Insect cell-derived	Yeast-derived	KHC (1–379)	KHC (1–560)
<b>ATP</b>				
Plus-end motility ( $\mu\text{m min}^{-1}$ )	$0.71 \pm 0.23$	$0.64 \pm 0.21$	$0.27 \pm 0.04$	$16.4 \pm 2.5$
Plus-end shorten ( $\mu\text{m min}^{-1}$ )	$0.39 \pm 0.19$	$0.12 \pm 0.05$	$0.00 \pm 0.00$	ND <sup>a</sup>
Minus-end shorten ( $\mu\text{m min}^{-1}$ )	$0.00 \pm 0.01$	$0.00 \pm 0.00$	$0.00 \pm 0.00$	ND
<i>n</i>	98	50	59	60
<b>AMP-PNP</b>				
Plus-end motility ( $\mu\text{m min}^{-1}$ )	$0.00 \pm 0.00$	$0.02 \pm 0.09^b$	$0.00 \pm 0.00$	$0.00 \pm 0.00$
Plus-end shorten ( $\mu\text{m min}^{-1}$ )	$0.07 \pm 0.03$	$0.06 \pm 0.03$	$0.00 \pm 0.00$	ND
Minus-end shorten ( $\mu\text{m min}^{-1}$ )	$0. \pm 0.01$	$0.00 \pm 0.01$	$0.00 \pm 0.00$	ND
<i>n</i>	50	24	59	60

Rates are presented as the mean  $\pm$  s.d. <sup>a</sup>Not determined. <sup>b</sup>Only one of 24 microtubules displayed a detectable movement.

microtubules, raised the possibility that Kip3p may have a novel combination of biochemical activities — plus end-directed motility and microtubule depolymerizing activity.

### Kip3p is a plus end-directed motor

Full-length Kip3p was expressed and purified from both insect cells and yeast by orthogonal purification strategies (see Methods). With each purification strategy, a fairly high yield of pure protein was obtained (as judged by Coomassie or silver stained gels; Fig. 2a, b). The Kip3p protein obtained from both sources migrated as a single band on SDS-PAGE at the expected molecular mass.

To determine whether Kip3p is capable of directed motility, microtubule-gliding assays were performed with Kip3p obtained from either source (Fig. 2c). In both cases, Kip3p adhered to the surface of the flow-cell and caused microtubules to bind and glide with similar velocities ( $0.6\text{--}0.7 \mu\text{m min}^{-1}$ ; Table 1). With two-colour polarity-marked microtubules<sup>28</sup>, we determined that Kip3p translocated towards the microtubule plus end (Fig. 2c and see Supplementary Information, Movies 3, 4). Notably, the Kip3p-driven microtubule-gliding velocities observed *in vitro* were somewhat slower relative to Kip3p-3YFP speckle analysis *in vivo*. This may reflect specific conditions of the *in vitro* assay or possibly Kip3p regulation *in vivo*. Alternately, an intrinsic affinity of Kip3p for the plus end, as suggested by Kip3p localization *in vivo*, may impede the progression of microtubules during gliding assays. Microtubule polarity was confirmed using recombinant fragments of kinesin heavy chain (KHC; Table 1). Similarly to other motile kinesins, Kip3p motor activity was blocked by the addition of the nonhydrolyzable ATP analogue AMPPNP. Therefore, consistent with data on *Drosophila* Klp67A<sup>16</sup>, Kip3p is a plus end-directed microtubule motor.

### Kip3p promotes plus end-specific microtubule depolymerization

In addition to gliding, Kip3p induced microtubule destabilization (Table 1). In the gliding assays described above, it was observed that shortening occurred only at the microtubule plus end. To characterize the microtubule depolymerization associated with Kip3p in conditions where the concentration of Kip3p could be more easily controlled, we developed an assay where biotin-modified microtubules were adhered to the surface of the reaction chamber, enabling combination of defined amounts of tubulin polymer and Kip3p. For this assay, single-colour bright-dim segmented microtubules were used, which enabled the identification of the plus end as the longer, dimly labelled, end<sup>28</sup>.

When Kip3p was added to immobilized microtubules, shortening still occurred. Furthermore, time-lapse microscopy revealed that the shortening was restricted to the plus end and occurred progressively (Fig. 3a and Supplementary Information, Movies 5–7). The rate of plus-end depolymerization increased with the concentration of Kip3p added to the reaction, while shortening at the minus end remained negligible (Fig. 3b). This microtubule depolymerization was dependent on Kip3p — the same preparations of guanosine-5' [ $\alpha$ ,  $\beta$ -methylene]triphosphate (GMPCPP)-stabilized microtubules<sup>29</sup> did not shorten in the absence of Kip3p or on addition of conventional kinesin (Fig. 3b and data not shown). Furthermore, very similar plus end-specific microtubule depolymerization was observed with Kip3p purified from either insect or yeast cells (Fig. 3a, b). In contrast, when an identical concentration of the *Xenopus* depolymerizing kinesin MCAK was used, the microtubule ends shortened ~sixfold faster than with Kip3p ( $0.35$  versus  $0.06 \mu\text{m min}^{-1}$ ;  $10 \mu\text{M}$  kinesin). As expected, MCAK-mediated depolymerization occurred at similar rates from both ends of the microtubule, such that the comparable MCAK concentration was also depolymerizing twice the number of microtubule ends (Fig. 3c and see Supplementary Information, Movie 8)<sup>30</sup>. Whereas AMPPNP completely blocked Kip3p-mediated microtubule gliding, it attenuated, but did not eliminate, microtubule destabilization (Fig. 3b). As discussed below, this may reflect common mechanistic features of kinesin-8 and kinesin-13 family members. Thus, Kip3p is both a plus end-directed motor and a plus end-specific microtubule depolymerase.

### Kip3p ATPase activity and tubulin dimer binding

We next explored the mechanism by which Kip3p depolymerizes microtubules by comparing the properties of Kip3p to those of kinesin-13 proteins. The non-motile kinesin-13 proteins (including MCAK) depolymerize microtubules by binding to terminal tubulin subunits<sup>5</sup>. Unlike conventional kinesins, the ATPase activity of MCAK is activated by tubulin dimers (unpolymerized tubulin)<sup>31</sup> and MCAK forms a nucleotide-sensitive complex with tubulin dimers<sup>30</sup>. Like motile kinesins, Kip3p possessed a low-level ATPase activity that was activated by microtubules (Fig. 4a). Strikingly, the Kip3p ATPase activity was also activated in a concentration-dependent manner by tubulin dimers (Fig. 4a). This tubulin-activation of Kip3p ATPase activity was strong, but less pronounced than that of microtubules. Additionally, sedimentation assays confirmed that this activity was not due to contaminating microtubules or short oligomers (see Supplementary Information, Fig. S2).

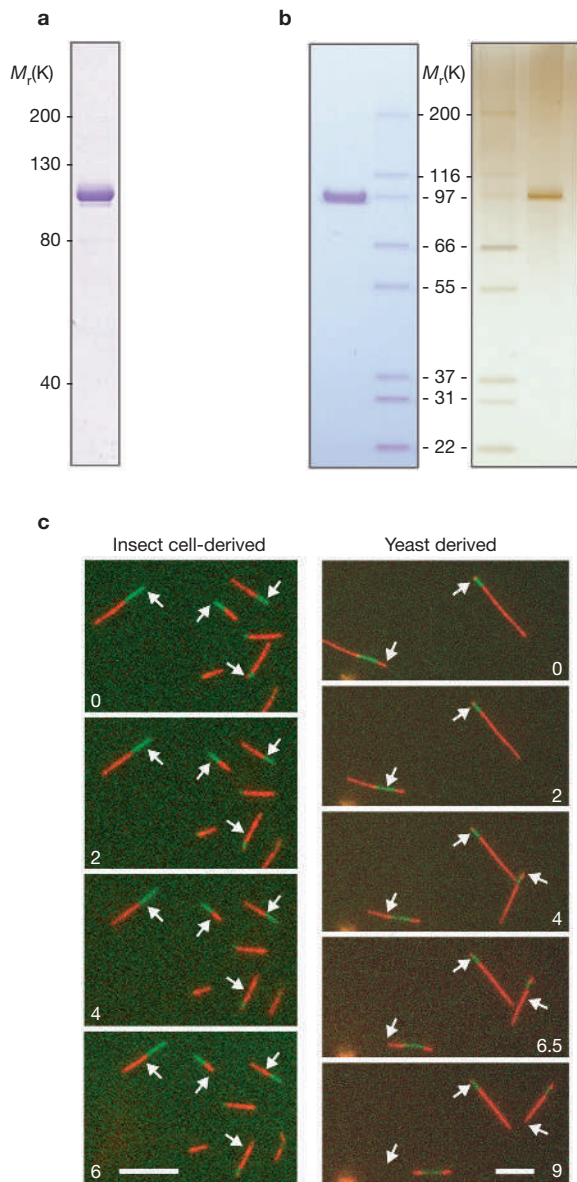


**Figure 2** Kip3p is a plus end-directed motor. **(a)** Coomassie-stained gel with 2  $\mu\text{g}$  purified Kip3p protein produced in insect cells. **(b)** Coomassie-stained (left, 2  $\mu\text{g}$  Kip3p) or silver-stained (right, 0.1  $\mu\text{g}$  Kip3p) gels with purified Kip3p protein produced in yeast. **(c)** Gliding assays showing the plus end-directed motility of Kip3p. The minus end of the microtubule is green and the plus end is red. Panels represent time-lapse images and numbers represent elapsed time (min). Arrows mark the minus end starting position of selected microtubules. The scale bars represent 5  $\mu\text{m}$ .

We next determined whether Kip3p, like MCAK, forms a nucleotide-sensitive complex with dimeric tubulin. In the presence of the nonhydrolyzable analogue AMPPNP, Kip3p did indeed form a complex with tubulin dimers (Fig. 4b). However, unlike MCAK, Kip3p also formed a robust complex with tubulin dimers after incubation with ATP (Fig. 4b). Under the higher salt conditions required for gel filtration (250 mM NaCl), the tubulin-activated ATPase of Kip3p was inhibited by  $\sim 80\%$  (see Supplementary Information, Fig. S3). Thus, at steady-state rates Kip3p hydrolyzed  $<10\%$  of the available ATP before gel filtration and could still interact with tubulin in the ATP-bound state. In contrast, when excess ADP was added (see Methods), Kip3p did not interact with

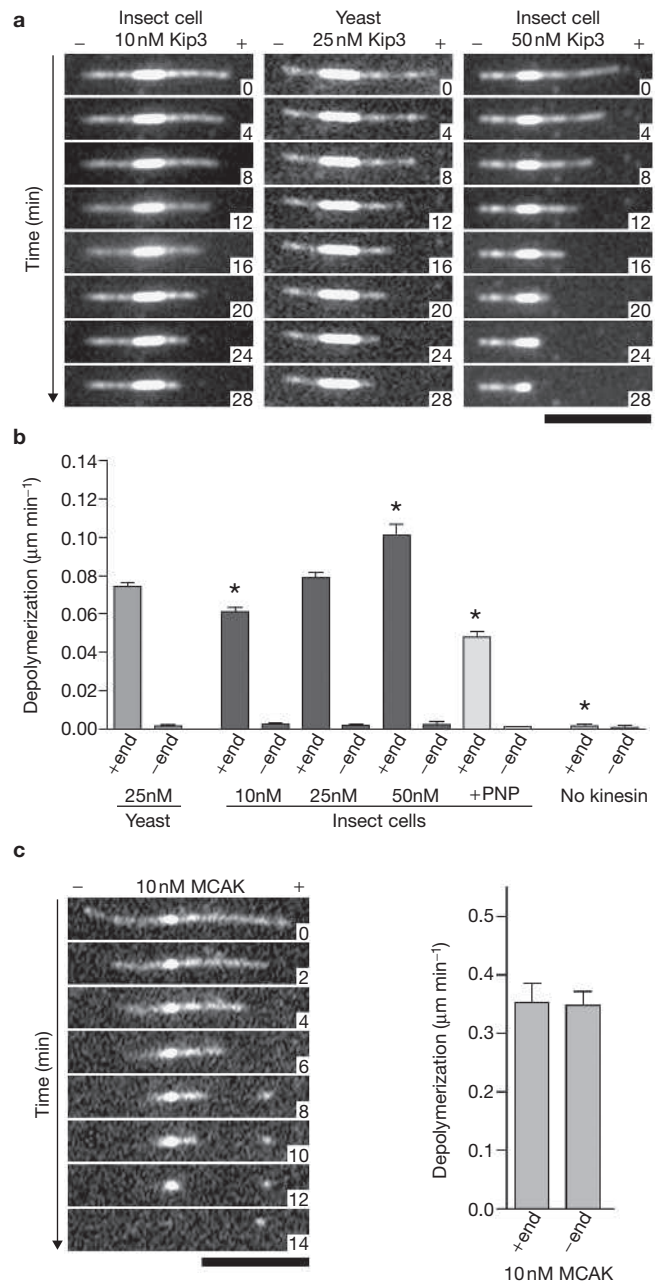


**Figure 3** Plus end-specific depolymerase activity of Kip3p. **(a)** Time-lapse imaging demonstrating concentration-dependent progressive shortening exclusively from the microtubule plus end by Kip3p. GMPPCP-stabilized, bright-dim segmented fluorescent microtubules (long dim ends are the plus end, 100 nM tubulin) were attached to the surface of a flowcell in the presence of the indicated amount of Kip3p (purified from the indicated source). **(b)** Plus end-specific depolymerization rates induced by different concentrations of Kip3p from yeast or insect cells ( $n = 94$  for 25 nM yeast-derived Kip3p and  $n = 106, 98$  and  $36$  for 10 nM, 25 nM and 50 nM insect cell-derived Kip3p, respectively;  $n = 82$  for 25 nM insect cell-derived Kip3p plus 2 mM AMPPNP;  $n = 34$  for no kinesin). +PNP indicates the AMPPNP treated sample. The experimental design is as in **a**. The error bars represent the s.e.m.  $*P < 0.001$  for plus-end depolymerization rate compared with 25 nM insect cell-derived Kip3p. **(c)** Control assays demonstrate *Xenopus* MCAK induces equivalent depolymerization of both ends of the microtubule ( $n = 25$ ). The scale bars represent 5  $\mu\text{m}$ .

**Table 2** Dynamic instability of cytoplasmic microtubules *in vivo*

	Wild type	<i>kip3Δ</i>		Wild type	<i>kip3Δ</i>
<b>Growth rate (<math>\mu\text{m min}^{-1}</math>)</b>			<b>Growth duration (s)</b>		
Overall	1.29 $\pm$ 0.40 (33)	1.21 $\pm$ 0.38 (66)	Overall	53 $\pm$ 19 (33)	115 $\pm$ 66 (66)**
G1	1.30 $\pm$ 0.46 (9)	1.27 $\pm$ 0.41 (17)	G1	46 $\pm$ 21 (9)	95 $\pm$ 54 (17)*
Pre-anaphase	1.21 $\pm$ 0.37 (17)	1.17 $\pm$ 0.36 (28)	Pre-anaphase	59 $\pm$ 17 (17)	126 $\pm$ 68 (28)**
Anaphase	1.50 $\pm$ 0.36 (7)	1.22 $\pm$ 0.40 (21)	Anaphase	48 $\pm$ 18 (7)	118 $\pm$ 70 (21)*
<b>Shortening rate (<math>\mu\text{m min}^{-1}</math>)</b>			<b>Shortening duration (s)</b>		
Overall	1.91 $\pm$ 0.69 (27)	2.82 $\pm$ 0.95 (48)**	Overall	44 $\pm$ 15 (27)	62 $\pm$ 34 (48)*
G1	1.98 $\pm$ 0.93 (5)	2.60 $\pm$ 1.03 (10)	G1	47 $\pm$ 14 (5)	68 $\pm$ 52 (10)
Pre-anaphase	1.87 $\pm$ 0.68 (15)	2.98 $\pm$ 0.85 (22)**	Pre-anaphase	46 $\pm$ 16 (15)	56 $\pm$ 19 (22)
Anaphase	1.96 $\pm$ 0.66 (7)	2.74 $\pm$ 1.05 (16)	Anaphase	37 $\pm$ 13 (7)	66 $\pm$ 37 (16)
<b>Catastrophe frequency (<math>\text{min}^{-1}</math>)</b>			<b>Rescue frequency (<math>\text{min}^{-1}</math>)</b>		
Overall	0.48 (21)	0.27 (39) <sup>a</sup>	overall	0.97 (19)	0.43 (21) <sup>a</sup>
G1	0.35 (4)	0.32 (10) <sup>a</sup>	G1	1.28 (5)	0.35 (4) <sup>a</sup>
Pre-anaphase	0.56 (12)	0.23 (15) <sup>a</sup>	Pre-anaphase	0.88 (10)	0.39 (8) <sup>a</sup>
Anaphase	0.45 (5)	0.29 (14) <sup>a</sup>	Anaphase	0.94 (4)	0.51 (9) <sup>a</sup>
<b>Dynamicity (dimers <math>\text{s}^{-1}</math>)</b>			<b>Time spent growing (percentage)</b>		
Overall	33.5	42.5	Overall	46.2	65.3
G1	30.6	42.5	G1	44.9	63.4
Pre-anaphase	35.8	42.4	Pre-anaphase	51.4	68.3
Anaphase	30.8	42.1	Anaphase	36.6	62.6
<b>Time spent in shortening (percentage)</b>			<b>Time spent attenuated (percentage)</b>		
Overall	30.9	25.4	Overall	22.9	9.4
G1	25.3	26.9	G1	29.8	9.7
Pre-anaphase	34.9	23.7	Pre-anaphase	13.8	8.1
Anaphase	27.9	26.6	Anaphase	35.5	10.9

For *kip3Δ*, a total of 54 microtubules from 37 different cells comprising 194 min of total microtubule lifetime were analysed. For wild-type, a total of 20 microtubules from 14 different cells comprising 63 min of total microtubule lifetime were analysed. Transition frequencies and percent time in each phase were determined for the entire population of microtubules. Rates and durations are reported as the mean  $\pm$  s.d. The number of events is in parentheses. \* $P < 0.02$ , \*\* $P < 0.001$ , <sup>a</sup>The variance for transition frequencies was not determined because transitions did not occur strictly stochastically; global transition frequencies differed from those measured at the cortex (see Fig. 6).

tubulin by gel filtration chromatography (Fig. 4b), demonstrating that the interaction is linked to the nucleotide status of the motor domain. Taken together, these experiments demonstrate that Kip3p has common biochemical properties with MCAK and suggest that Kip3p may depolymerize microtubules by a similar mechanism.

**Kip3p microtubule dynamics and spindle positioning** Genetically, budding yeast has two spindle positioning mechanisms. The first depends on dynein–dynactin and the second depends on the +TIP Kar9p. This latter mechanism involves interactions between microtubule plus-end factors (Bim1p and Kar9p) and a type V myosin (Myo2p) that transports Kar9p–Bim1p, together with the ends of microtubules, along actin cables to the bud tip<sup>32,33</sup>. Genetic analysis has shown that Kip3p is required for the Kar9-dependent mechanism, however, the role of Kip3p in this process is not clear<sup>8–10</sup>. Kip3p could function in: the regulation of myosin-dependent transport of plus ends to the bud; the coupling of cortically-associated plus-end depolymerization (capture–shrinkage<sup>34</sup>); the regulation of microtubule dynamics; or some combination of these functions.

The role of Kip3p in spindle positioning was characterized at each step of the process. First, we determined whether Kip3p is required for the myosin-dependent transport of cytoplasmic microtubule plus ends into the bud. When synchronized *kip3Δ* cultures entered the cell cycle

(release from a late anaphase block), microtubules robustly established interactions with the bud tip (Fig. 5a). Live imaging of GFP–tubulin expressing cells showed that at least one microtubule occupied the bud 26% of the time in wild-type cells (9 cells monitored for 56 min total). Likewise, in *kip3Δ* cells, at least one microtubule occupied the bud 36% of the time (9 cells monitored for 62 min total). Furthermore, as in wild-type cells, bud-directed sweeping movements of microtubule plus ends were also observed in *kip3Δ* cells (Fig. 5b). Thus, Kip3p is not required for myosin-dependent transport of microtubule plus ends.

Second, we determined whether Kip3p has a role in coupling microtubule attachment and depolymerization during cortical interaction, as has been suggested for the kinesin-14 motor Kar3p during mating<sup>35</sup>. Capture–shrinkage events were still readily observed at the bud tip in *kip3Δ* cells (Fig 5c; 3 events during 462 s of microtubule contact with bud tip for wild-type cells; 3 events during 1122 s for *kip3Δ* cells). Although the frequency of capture–shrinkage was slightly reduced in *kip3Δ* cells, the events observed seemed to be qualitatively similar to wild-type cells.

Third, we characterized microtubule dynamics in wild-type and *kip3Δ* cells in detail (Table 2). Consistent with biochemical analysis, deletion of *KIP3* produced a 44% reduction in catastrophe frequency. Loss of Kip3p also had a striking effect on microtubule pausing — the amount of time microtubules spent paused was reduced by 59%

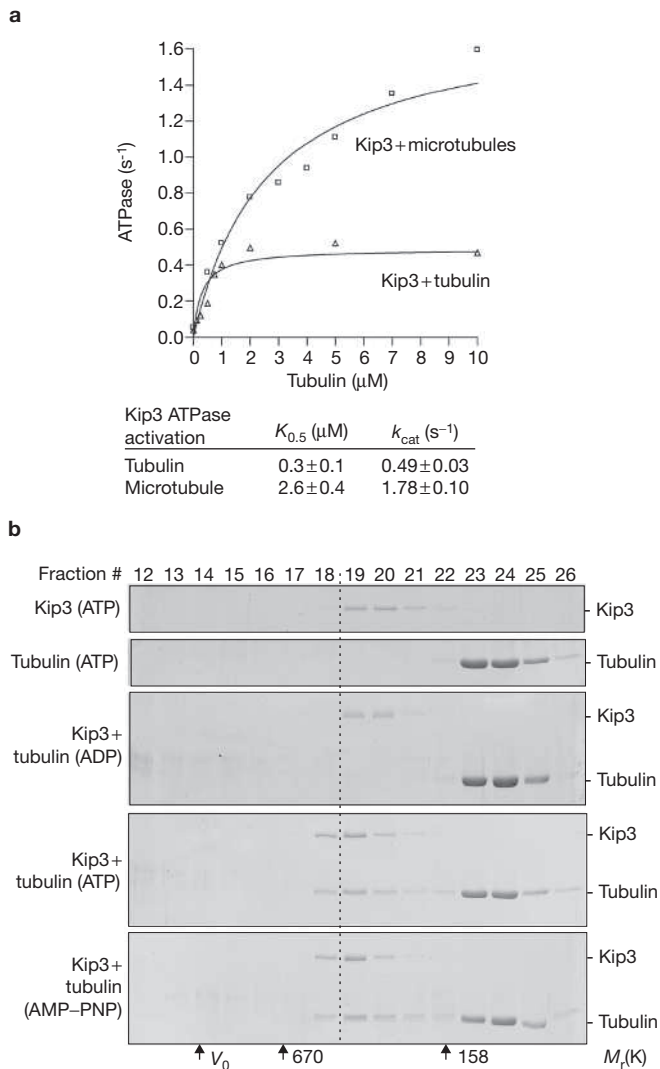


**Figure 4** Kip3p has tubulin dimer-activated ATPase activity and forms a nucleotide-dependent complex with tubulin dimers. **(a)** Microtubule and tubulin-activated ATPase activity of Kip3p. The steady-state ATPase rate of 200 nM insect cell-derived Kip3p was determined with increasing concentrations of Taxol-stabilized microtubules (squares) or GDP-tubulin (triangles). The data points represent the ATPase activity determined for a single experiment. The curves represent the rates from multiple experiments fit to the Michaelis-Menten equation (tubulin,  $n = 3$ ; microtubules,  $n = 4$ ). Kip3p had an intrinsic ATPase rate of  $0.07 \pm 0.02 \text{ s}^{-1}$ . The tubulin-activated ATPase activity did not result from contaminating microtubules or oligomers (see Supplementary Information, Fig. S2). **(b)** Nucleotide-dependent complex of Kip3p with unpolymerized tubulin. Mixtures of 2  $\mu\text{M}$  Kip3p and 5  $\mu\text{M}$  tubulin dimer were incubated with the indicated nucleotide before analytical gel filtration. Column fractions were examined by Coomassie-stained SDS-PAGE. The elution profiles of both proteins in the ADP-containing mixture (Apyrase + ADP; see Methods) were identical to the elution profiles when each protein was analysed individually. The void volume ( $V_0$ ) and elution volume for reference proteins are marked by arrows.

compared with microtubules in wild-type cells. Factoring in effects on both growth and shrinkage rates, the decreased pause time was almost balanced by a 41% increase in the amount of time microtubules spent growing relative to wild-type cells, resulting in an overall increase in dynamicity (Table 2). Taken together, these data explain why loss of Kip3p increases microtubule length, as has been observed in budding yeast and other eukaryotic cell types<sup>8-12,15,18</sup>.

Kip3p affected other parameters of dynamic instability aside from catastrophes. Once they started shortening, microtubules in *kip3Δ* cells depolymerized at a significantly faster velocity than the microtubules in wild-type cells (Table 2;  $P < 0.001$ ). Additionally, during these periods of accelerated disassembly, the frequency of rescue was reduced by 56% relative to the rescue frequency in wild-type cells. As discussed in more detail below, the complex effect of Kip3p on microtubule dynamics may reflect direct effects of multiple Kip3p activities or indirect effects on other +TIPs.

To better understand how Kip3p-dependent control of microtubule dynamics impacted on spindle positioning, microtubule-cortical interactions were characterized in detail in *kip3Δ* cells. Consistent with data from other systems<sup>36-38</sup>, in wild-type cells the frequency of catastrophe at the cell cortex was approximately fourfold higher than the global catastrophe frequency (Fig. 6a). The frequency of microtubule catastrophe at the cell cortex was decreased by 60% in *kip3Δ* cells. This effect was further enhanced at the bud tip (Fig. 6a). Correspondingly, the dwell time of microtubules at the cortex was increased approximately threefold in *kip3Δ* cells by comparison with wild-type cells (Fig. 6b;  $P < 0.001$  for both).

Kip3p also had a notable influence on the balance between the growing versus pausing of cortical-associated microtubules (Fig. 6c). When microtubules in wild-type cells were in contact with the bud tip, there was a pronounced drop in the amount of time they spent either growing or shortening, and a dramatic increase (from 11 to 76%) in the time they spent in a paused state. In contrast, microtubules contacting the bud tip spent only 16% of their time paused in *kip3Δ* cells and continued growing during 71% of the time.

Together, our analysis of microtubule dynamics suggests the hypothesis that spindles are mis-positioned in *kip3Δ* cells because attached microtubules grow inappropriately, pushing preanaphase spindles away from their normal position near the bud neck. Consistent with this hypothesis, during spindle positioning in *kip3Δ* cells, prolonged microtubule elongation at the bud tip was frequently observed, which forced the SPB to the extreme opposite side of the mother cell (Fig 6d; see Supplementary Information, Movie 9). Occasionally, the excessive polymerization of bud tip-associated microtubules in *kip3Δ* cells resulted in microtubule buckling, breakage and subsequent depolymerization. This contrasted with the situation in wild-type cells, where the SPBs remained positioned near the bud neck while microtubules repeatedly interacted with the bud tip over several minutes (Fig. 6d; see Supplementary Information, Movie 10). Thus, Kip3p is a crucial regulator of the dynamics and length of cortically attached microtubules.

To directly test the hypothesis that preanaphase spindles in *kip3Δ* cells are mispositioned by the excessive growth of bud tip-associated microtubules, images of cells were categorized during Kar9-dependent spindle positioning according to whether microtubule plus ends were in contact with the bud tip and the position of the unseparated SPBs relative to the bud neck was subsequently determined. In wild-type cells, the average distance between the SPB and bud neck was independent of whether microtubules were in contact with the bud tip or not (Fig. 6e). However, in *kip3Δ* cells the position of the SPB was strongly influenced by microtubule bud-tip attachment: the SPB was appropriately positioned closer to the bud neck if microtubules failed to contact the bud tip, but the SPB was strikingly mispositioned when microtubules did contact the bud tip (SPB to neck = 1.9  $\mu\text{m}$  without versus 2.6  $\mu\text{m}$  with microtubule contact;  $P = 0.02$ ). Thus, the function of Kip3p as a regulator of the dynamics of microtubules attached to the bud tip explains its role in positioning the mitotic spindle.

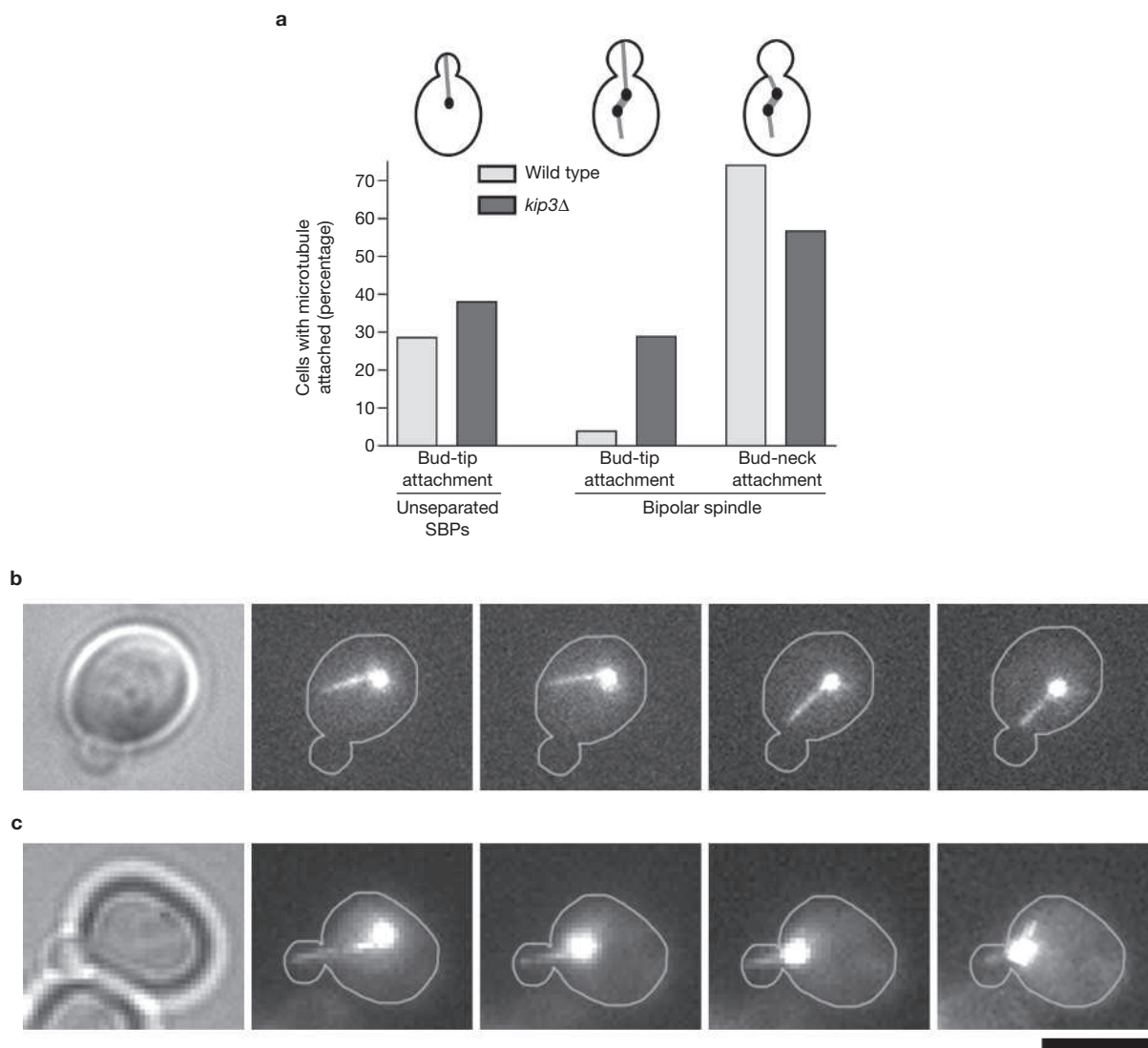


**Figure 5** Normal microtubule orientation and capture–shrinkage in G1–S *kip3Δ* cells. **(a)** The percentage of cells with a microtubule attached to the bud tip or bud neck after release from a late anaphase block (*cdc15-2*, 37 °C). Cells with unseparated SBPs were scored 80 min after release and cells with bipolar spindles were scored 100 min after release. Wild-type,  $n = 196$  and 77 and *kip3Δ*,  $n = 271$  and 90, for cells with unseparated SBPs and bipolar spindles, respectively. Similar results were obtained from

the analysis of unsynchronized cells (data not shown). **(b)** Microtubule orientation in *kip3Δ* cells. Images from a time-lapse experiment illustrating normal microtubule orientation toward the bud in a G1–S phase *kip3Δ* cell. Microtubules were labelled with GFP–Tub1p. Time between fluorescence images is 6 s. **(c)** Images from a time-lapse experiment illustrating a normal cortical capture–shrinkage event in a G1–S phase *kip3Δ* cell. Time between fluorescence images is 15 s. The scale bar represents 5  $\mu$ M.

## DISCUSSION

Here, we report that Kip3p has a unique combination of activities for a kinesin motor: a plus end-specific depolymerase activity and plus end-directed motility. *In vivo*, Kip3p-tracked microtubule plus ends and dynamic imaging suggests that the motor activity targets the depolymerase activity to the plus end. During microtubule–cortical interactions, Kip3p dramatically induced microtubule pausing and raised the catastrophe frequency, thus explaining the requirement for Kip3p for positioning of mitotic spindles during asymmetric cell division in budding yeast.

We found that the ATPase activity of Kip3p is activated by tubulin dimers and that Kip3p forms a nucleotide-dependent complex with tubulin. These characteristics are associated with kinesin-13 depolymerases<sup>5</sup>. However, it was recently demonstrated that the plus end-directed chromokinesin Xklp1 also possesses similar characteristics<sup>39</sup>. All of these kinesins directly affect microtubule dynamics, although in

the case of Xklp1 the effect is attenuated dynamic instability rather than destabilization<sup>39</sup>. The structure of kinesin-13 proteins has led to appealing models that explain the mechanism of their depolymerase activity<sup>22,23</sup>. Interestingly, at the sequence level, kinesin-8 proteins lack the kinesin-13-specific elements proposed to mediate depolymerization. For example, the residues that form an extension of the microtubule-binding helix  $\alpha 4$  in KIF2C (a kinesin-13) are not conserved in kinesin-8 proteins. Also, kinesin-8 proteins lack the LysValAsp (KVD) motif inserted into Loop2 — another important part of the proposed kinesin-13 microtubule-binding surface. Whether the kinesin-8 insertions at this site are structurally similar has yet to be determined. Based on the proposed mechanism for kinesin-13 depolymerization, a similar interaction with tubulin dimers would not be predicted for a ‘walking’ kinesin, such as Kip3p. However, the activities of Xklp1 reveal that walking kinesins are capable of regulated interaction with tubulin dimers. Determining the structure of kinesin-8

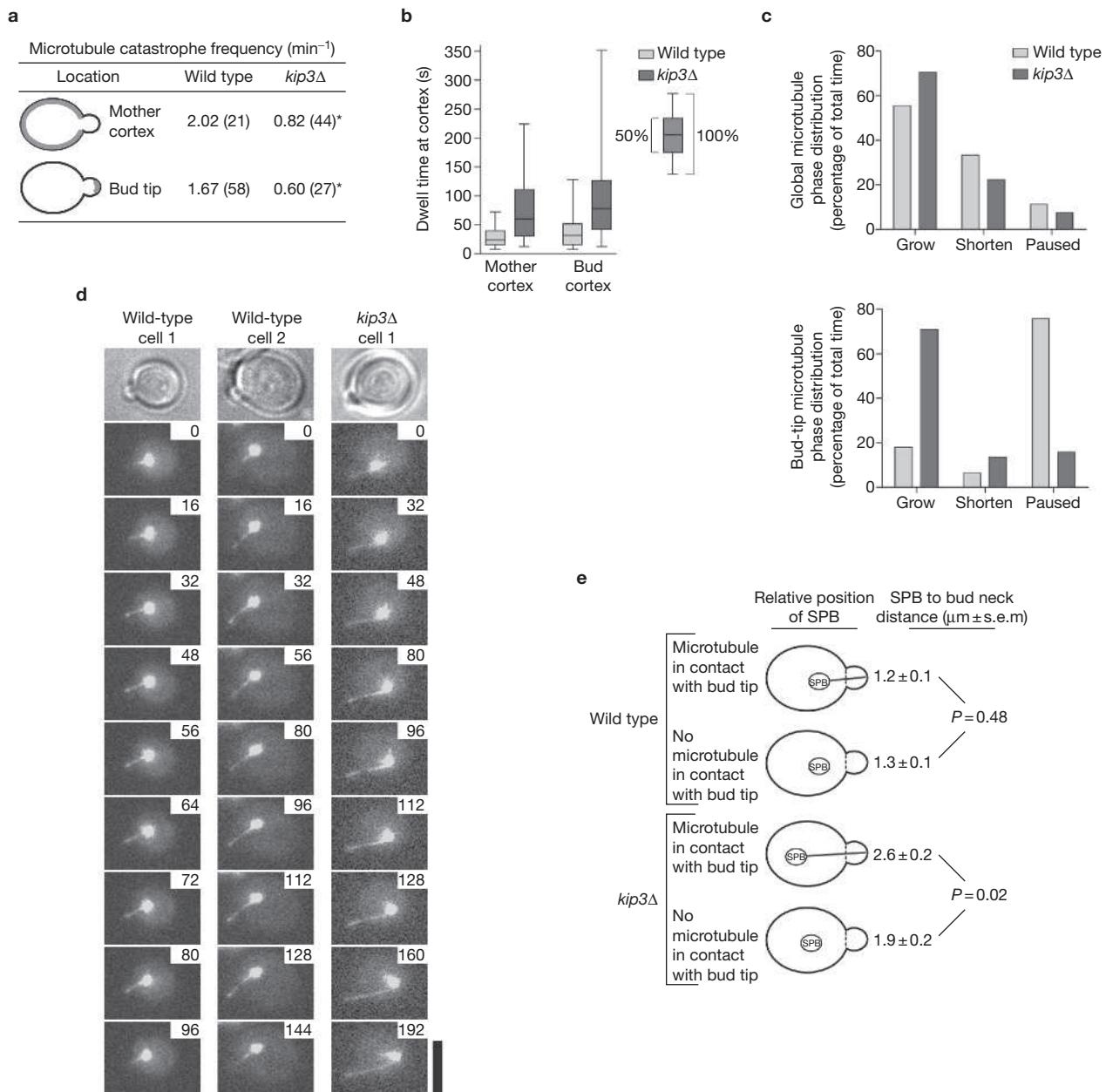


**Figure 6** Kip3p is required to position mitotic spindles as it is a critical regulator of the length of cortically attached microtubules. **(a)** Catastrophe frequencies at the cell cortex in small-budded *kip3Δ* or control cells. \* $P < 0.001$  compared to wild-type, assuming a Poisson distribution of catastrophes during microtubule contact with the cortex. The number of events is in parentheses. **(b)** Dwell times of microtubule plus ends at the mother or bud (usually the bud tip) cortex in *kip3Δ* or control cells. Wild type,  $n = 21$  and 59; *kip3Δ*,  $n = 44$  and 27 for mother and bud tip cortical interactions, respectively. **(c)** Kip3p is required for pausing of microtubules on cortical contact. In wild-type cells, there was a sevenfold increase in the amount of time microtubules spend in a paused state. This effect was abolished in *kip3Δ* cells, where cortically attached microtubules spend most

of their time growing. Forty one microtubule–bud tip interactions comprising 1376 s and 26 interactions lasting 2388 s were analysed for wild-type and *kip3Δ* cells, respectively. The global phase distributions were calculated from small budded cells presented in Table 2. **(d)** Examples of cells illustrating the behaviours described in **c**. Microtubules are labelled with GFP–Tub1p. Microtubules in two wild-type cells exhibit  $>30$  s pauses on contact with the bud tip. A microtubule in a *kip3Δ* cell exhibits persistent growth over a 190 s interval after contact with the bud tip. **(e)** Schematic representation of spindle positioning relative to bud neck in small budded cells. In *kip3Δ* cells, spindles are strikingly mispositioned only if a cytoplasmic microtubule contacts the cortex. Wild type,  $n = 10$  and 27; *kip3Δ*,  $n = 12$  and 29 for the presence and absence of microtubule bud-tip contact, respectively.

destabilized microtubule minus ends during motility assays<sup>6</sup>. However, it was recently demonstrated that a fragment of the accessory protein Cik1p can target Kar3p to the microtubule plus end, with an accompanying plus end depolymerase activity<sup>7</sup>. Kar3p and kinesin-13 proteins seem to differ mechanistically because, unlike MCAK, Kar3p-mediated depolymerization is tightly coupled to ATP hydrolysis, the ATPase activity of Kar3p

proteins, and comparing them to kinesin-13 family members, should provide insights into the mechanisms by which kinesins can function as depolymerases.

Kip3p is the second kinesin characterized that has both motility and depolymerase activity. Kar3p (a kinesin-14 family member) is a minus-end motor and it was initially reported that the motor domain of Kar3p

920

NATURE CELL BIOLOGY VOLUME 8 | NUMBER 9 | SEPTEMBER 2006

©2006 Nature Publishing Group

is not activated by tubulin dimers and Kar3p did not detectably bind tubulin<sup>7</sup>. Furthermore, in contrast with kinesin-13 proteins, GMPCPP-stabilized microtubules are not effective substrates for Kar3p depolymerization<sup>7</sup>. Thus, our results also imply fundamental mechanistic differences between Kar3p (a kinesin-14) and Kip3p (a kinesin-8).

The mechanism of Kip3p accumulation at microtubule tips *in vivo* may be due to either an intrinsic affinity for the plus end or be mediated through other plus end-binding factors. Although kinesin-13 proteins can rapidly target microtubule ends by a diffusional mechanism *in vitro*<sup>31</sup>, *in vivo* both kinesin-13 proteins and Kar3p use accessory factors to target or maintain interactions with the plus end<sup>35,40,41</sup>. In contrast, Kip3p is unique in that it possesses plus end-directed motility and therefore can transport its own destabilizing activity towards the microtubule tip. Indeed, our speckle analysis suggests that Kip3p motility is an efficient mode of delivery because Kip3p speckles were frequently observed travelling the entire length of the microtubule. This may provide a mechanism to enrich Kip3p at its site of action, the microtubule plus end, even if the cytoplasmic concentration of Kip3p is low. It will be interesting to determine how Kip3p accumulates at the plus end and to define the relationship between the Kip3p walking and depolymerizing activities.

In living cells, the intrinsic dynamicity of microtubules must be modulated for functions in different local environments. In budding yeast, the requirement of Kip3p for cytoplasmic microtubule behaviour is particularly evident during cortical interactions, when Kip3p prevents microtubule growth and strikingly elevates the frequency of catastrophe. The effect on catastrophes is enhanced at the bud tip where the actin-rich environment may stabilize microtubules<sup>42,43</sup>. Similar regulation may take place in other organisms. For instance, nuclear positioning in *Schizosaccharomyces pombe* involves the regulated catastrophe of microtubules at the cell tips<sup>36,37</sup>. Deletion of the Kip3p homologues in *S. pombe*, Klp5 or Klp6, results in cells with long microtubules that curve around the tips of cells<sup>11,12</sup>, suggesting a conserved function for kinesin-8 proteins during microtubule-cortical interactions. In *Caenorhabditis elegans* embryos, the duration of microtubule-cortical interaction is differentially regulated between microtubules contacting the anterior versus posterior cortex<sup>44</sup>. Similar to our observations, it has been suggested that growing microtubules convert to a paused state on cortical contact in *C. elegans*<sup>44</sup>. Although it is unclear whether a functional kinesin-8 homologue exists in *C. elegans*, these findings nevertheless underscore the importance of altering microtubule dynamics during cortical contact.

The biochemical properties of Kip3p identified here are consistent with the *in vivo* role at cytoplasmic and kinetochore microtubule plus ends. Inhibiting microtubule growth and promoting catastrophe may explain the recent finding that Kip3p is needed for synchronous and efficient movement of kinetochores during anaphase segregation<sup>18</sup>. However, we also uncovered effects on microtubule dynamics that suggest additional complexities. Principally, in the absence of Kip3p, microtubules depolymerized at a faster rate and experienced fewer rescues. This may occur because the absence of Kip3p alters the stoichiometry of other factors at the plus end, as we have previously shown for Bim1p, Bik1p and dynein<sup>4</sup>. Alternatively, based on the microtubule-stabilizing effects of Xklp1 (ref. 39), the accumulation of walking Kip3p near the depolymerizing plus end may stabilize the lattice, slow depolymerization and foster rescue. A similar effect on the rate of microtubule depolymerization was seen after inhibition of KCM1 (a kinesin-13) in PtK2 cells<sup>45</sup>.

Our findings explain the role of Kip3p in budding yeast spindle positioning. In the absence of Kip3p, unregulated microtubule growth, together with prolonged interactions at the bud tip, creates a pushing force that mispositions spindles oriented by the Bim1-Kar9-Myo2 system<sup>33</sup>. The data thus explains previous genetic results indicating that the consequences of Kip3p loss can be, at least partially, bypassed by the additional loss of another kinesin, Kip2p<sup>8-10</sup>: the hyperstabilized microtubules of Kip3p-deficient cells can be partially rectified by the destabilizing effects of Kip2p loss. Because Kip2p functions in the dynein-dependent spindle positioning pathway<sup>4</sup>, these results are consistent with our conclusion that the other major components of the Kar9-dependent positioning pathway remain functional without Kip3p.

The loss of kinesin-8 proteins in divergent cell types produces similar effects on microtubule length, indicating that the molecular functions reported here are likely to be conserved. Our studies reveal how the budding yeast kinesin-8 regulates microtubule dynamics during cortical interactions. Kinesin-8 proteins may function in a similar manner to control kinetochore dynamics during chromosome congression and segregation in yeast and other eukaryotic cells. □

*Note added in proof: a related manuscript by Varga et al. (Nature Cell Biol. 8, doi: 10.1038/ncb1462; 2006) is also published in this issue.*

## METHODS

**Strains and constructs.** Baculovirus strain DR681-Kip3 contains the full coding sequence of Kip3p with a 6×His affinity tag fused to the amino terminus. Plasmid pB2537 contains the full-length coding sequence for Kip3p with N-terminal 6×His and carboxy-terminal StrepII (Qiagen, Hilden, Germany) affinity tags cloned into pRS426. Plasmid pB2538, containing coding sequence for the C-terminal region of Kip3p fused to three tandem copies of YFP, was used to convert the endogenous loci of *KIP3* into *KIP3-3YFP*. All of the cloned *KIP3*, linker segments and affinity tags were verified by DNA sequencing.

Media and genetic techniques were as previously described<sup>46</sup>. Kip3p-3YFP fusion protein is functional as assayed by complementation of synthetic lethality with *dyn1Δ* (29 *KIP3-3YFP dyn1Δ* spores recovered from the analysis of 27 tetrads; *KIP3-3YFP dyn1Δ* strains grew indistinguishably from wild-type controls at 16, 24, 30 and 37 °C). Yeast strains were of S288C background. The details of plasmid and strain construction are available upon request.

**Protein expression and purification.** To purify Kip3p from insect cells (using baculovirus expression), cells were lysed and the soluble fraction obtained by centrifugation for 30 min at 100,000g. His-Kip3p was purified by Ni<sup>++</sup> affinity chromatography followed by application to an UNO S ion exchange column and then gradient elution. The purified protein was concentrated, dialysed cleared at 150,000g and snap-frozen in liquid nitrogen. Detailed descriptions are provided in the Supplementary Information, Methods.

To obtain Kip3p expressed from pB2537 (*GAL1::6×His-KIP3-StrepII*) in yeast cells, a 10 g cell pellet was washed, lysed, sonicated for 30 s and cleared with a 45 min spin at 100,000g. 6×His-Kip3p-StrepII was purified by tandem affinity chromatography using Ni-NTA followed by Strep-Tactin resin (Qiagen). The purified protein was stored as above. Concentrations reported refer to monomeric Kip3p. Detailed descriptions are provided in the Supplementary Information, Methods.

Purified His-MCAK (*Xenopus* XKCM1) and KHC-6×His (amino acids 1-560) protein was a generous gift from R. Ohi and T. Mitchison (Harvard Medical School, Boston, MA). The GST-KHC motor domain (amino acids 1-379) fusion protein, although slower than larger KHC fragments, retains plus end-directed motility (Cytoskeleton, Inc., Denver, CO).

**Preparation of tubulin and stabilized microtubules.** Stabilized microtubules (from phosphocellulose-purified bovine tubulin) were freshly prepared on the day of each experiment. Before preparing GMPCPP-stabilized assembly mixtures or N-ethylmaleimide-modified (NEM) tubulin, the purified tubulin was cycled by polymerization and depolymerization, and then cleared by ultracentrifugation. NEM-tubulin was prepared as previously described<sup>47</sup>. Bright-dim segmented

(without NEM–tubulin) and two-colour polarity marked (with NEM–tubulin) GMPCPP-stabilized microtubules were prepared by previously described methods<sup>28</sup>. Detailed descriptions of stabilized microtubule preparation are provided in the Supplementary Information, Methods.

**Motility and depolymerase assays.** Microtubule gliding assays were performed according to established methods<sup>48</sup> with minor modifications (see Supplementary Information, Methods for detailed descriptions). All washing and reaction mixtures contained an oxygen scavenging mix (OSM; 200 µg ml<sup>-1</sup> glucose oxidase, 35 µg ml<sup>-1</sup> catalase, 25 mM glucose and 70 mM β-mercaptoethanol). Images were recorded every 10–60 s. Microtubule velocities were determined for continuous movement over at least 2–4 min using the green–red interface on the microtubule as a reference.

To determine microtubule depolymerization rates, kinesin proteins were mixed with biotin-modified (1:200 molar ratio) microtubules and applied to anti-biotin coated perfusion chambers. Images were recorded every 30 s. Microtubules were scored for polarity if the plus-end segment was at least twice as long as the minus-end segment. Microtubule lengths were measured with respect to the bright–dim interface.

During the gliding assays, it was noted that microtubules consistently depolymerized several-fold faster compared with the biotin antibody-attached microtubules. Although the concentrations of bound Kip3p retained in the gliding assays were not known, this result suggests that the observed Kip3p depolymerization rates *in vitro* may be somewhat slowed for biotin-tethered microtubules. This tether may act to stabilize the microtubules and slow depolymerization.

In both KHC and Kip3 assays, 1–3 microtubules behaved with opposite apparent polarity (plus-end leading and minus-end shortening). These microtubules typically arose several hours after preparation of polarity-marked microtubules and are likely to result from annealing and/or breaking of microtubules during pipetting<sup>47</sup>. These microtubules were omitted from the rates presented.

**Gel filtration.** Kip3p (2 µM; insect cell-derived) and 5 µM tubulin were incubated for 15 min at room temperature in BRB80 (80 mM potassium PIPES, 1 mM EGTA, 1 mM MgCl<sub>2</sub> at pH 6.9) supplemented with 270 mM NaCl, 1 mM dithiothreitol (DTT), 50 µM GDP and 3 mM either ATP, AMPPNP or Apyrase plus ADP (see below) before separation on a 0.32 × 30 cm Superdex-200 FPLC column. The column was run in BRB80, 250 mM NaCl, 20 µM GDP and 200 µM of the same adenosine nucleotide. For stability, ATP was maintained in Kip3p purification and storage buffers. Full-length Kip3p required >250 mM NaCl for maximum solubility during gel filtration. Because the tubulin-activated ATPase activity of Kip3p was inhibited at high salt concentration (see Supplementary Information, Fig. S3), to deplete residual ATP carryover from purification buffers (~30 µM) the following procedure was used: Kip3p was first incubated with 0.15 units Apyrase for 7 min in BRB80 with 331 mM NaCl, followed by addition of 5 µM tubulin and 1.5 mM ADP (275 mM NaCl final) after 12 min incubation. Another 1.5 mM ADP was added 3 min before gel filtration. Equal fraction volumes were applied to each gel.

**Steady-state ATPase measurements.** Steady-state ATPase activity was measured using the previously described NADH-coupled system<sup>49</sup>. Measurements were determined using 200 nM Kip3p in 50 mM Tris–OAc at pH 7.5), 1 mM MgCl<sub>2</sub>, 1 mM DTT, 3 mM phospho(enol)pyruvate, 0.21 mM NADH and with 25 mM KCl, 1 mM ATP, 17 U ml<sup>-1</sup> pyruvate kinase, 19 U ml<sup>-1</sup> lactate dehydrogenase, 0.1 mg ml<sup>-1</sup> casein and varying concentrations of tubulin or 10 µM paclitaxel (Taxol)-stabilized microtubules. To verify that the enzyme-linked NADH oxidation was not rate-limiting, the concentration of Kip3p was increased up to threefold at the highest microtubule concentration, with a linear increase in steady-state ATPase readout, and the half-time for response after addition of 0.05 mM ADP was 20 s.

**Cell imaging, *in vivo* microtubule dynamics and cortical interactions.** Image acquisition and analysis was performed as previously described<sup>4</sup>. The images in Figs 1a and 5b–c represent maximum-intensity projections of 3D images. Global cytoplasmic microtubule dynamics were determined as previously described, with 3D image stacks acquired every 5–8 s<sup>50</sup>. Because in our previous experiments measurements of microtubule dynamics from 2D projections were nearly identical to measurements from 3D image stacks, 2D projections were used to measure length. To determine catastrophe frequency, only the time spent in growth and

pause phase was considered. For rescue frequency, only time shrinking was considered. For cortical interactions, a differential interference contrast (DIC) image was used to identify the cell cortex. The criteria applied for cortical interaction was that the plus end of the microtubule reached the cell cortex in the central fluorescence image and that the entire microtubule remained in focus, from the plus end to the SPB. The criteria applied for cortical catastrophe was that the tip of the microtubule shrank away from the cortex and remained in focus, with a concomitant decrease in SPB–tip length. For microtubule dynamics at the bud tip, at least three consecutive time points defined a growth–shrinkage–pause event. The distal third of small buds was considered the tip. *P* values were determined using Student's *t* test.

*Note: Supplementary Information is available on the Nature Cell Biology website.*

#### ACKNOWLEDGMENTS

We are grateful to K. Bloom, J. Huff, A. Murray, R. Ohi and A. Straight for providing reagents. We thank S. Gilbert, T. Mitchison, H. Sosa and members of the Pellman lab for discussion, and S. Buttery, N. Chandhok, S. Gilbert, M. Guillet and S. Yoshida for comments on the manuscript. M. Gupta was supported by a postdoctoral fellowship from the American Cancer Society (ACS; PF-05-025-01-CCG). D. Pellman was supported by a National Institutes of Health (NIH) grant (GM R0161345).

#### COMPETING FINANCIAL INTERESTS

The authors declare that they have no competing financial interests.

Published online at <http://www.nature.com/naturecellbiology/>

Reprints and permissions information is available online at <http://npg.nature.com/reprintsandpermissions/>

- Nogales, E. Structural insights into microtubule function. *Annu. Rev. Biochem.* **69**, 277–302 (2000).
- Sharp, D. J., Rogers, G. C. & Scholey, J. M. Roles of motor proteins in building microtubule-based structures: a basic principle of cellular design. *Biochim. Biophys. Acta* **1496**, 128–141 (2000).
- Busch, K. E., Hayles, J., Nurse, P. & Brunner, D. Tea2p kinesin is involved in spatial microtubule organization by transporting tip1p on microtubules. *Dev. Cell* **6**, 831–843 (2004).
- Carvalho, P., Gupta, M. L., Jr., Hoyt, M. A. & Pellman, D. Cell cycle control of kinesin-mediated transport of Bik1 (CLIP-170) regulates microtubule stability and dynein activation. *Dev. Cell* **6**, 815–829 (2004).
- Moore, A. & Wordeman, L. The mechanism, function and regulation of depolymerizing kinesins during mitosis. *Trends Cell Biol.* **14**, 537–546 (2004).
- Endow, S. A. *et al.* Yeast Kar3 is a minus-end microtubule motor protein that destabilizes microtubules preferentially at the minus ends. *EMBO J.* **13**, 2708–2713 (1994).
- Sproul, L. R., Anderson, D. J., Mackey, A. T., Saunders, W. S. & Gilbert, S. P. Cik1 targets the minus-end kinesin depolymerase kar3 to microtubule plus ends. *Curr. Biol.* **15**, 1420–1427 (2005).
- Cottingham, F. R. & Hoyt, M. A. Mitotic spindle positioning in *Saccharomyces cerevisiae* is accomplished by antagonistically acting microtubule motor proteins. *J. Cell. Biol.* **138**, 1041–1053 (1997).
- DeZwaan, T. M., Ellingson, E., Pellman, D. & Roof, D. M. Kinesin-related KIP3 of *Saccharomyces cerevisiae* is required for a distinct step in nuclear migration. *J. Cell. Biol.* **138**, 1023–1040 (1997).
- Miller, R. K. *et al.* The kinesin-related proteins, Kip2p and Kip3p, function differently in nuclear migration in yeast. *Mol. Biol. Cell* **9**, 2051–2068 (1998).
- West, R. R., Malmstrom, T., Troxell, C. L. & McIntosh, J. R. Two related kinesins, klp5+ and klp6+, foster microtubule disassembly and are required for meiosis in fission yeast. *Mol. Biol. Cell* **12**, 3919–3932 (2001).
- Garcia, M. A., Koonrugsa, N. & Toda, T. Two kinesin-like Kin I family proteins in fission yeast regulate the establishment of metaphase and the onset of anaphase A. *Curr. Biol.* **12**, 610–621 (2002).
- Gatt, M. K. *et al.* Klp67A destabilises pre-anaphase microtubules but subsequently is required to stabilise the central spindle. *J. Cell Sci.* **118**, 2671–2682 (2005).
- Goshima, G. & Vale, R. D. The roles of microtubule-based motor proteins in mitosis: comprehensive RNAi analysis in the *Drosophila* S2 cell line. *J. Cell Biol.* **162**, 1003–1016 (2003).
- Goshima, G., Wollman, R., Stuurman, N., Scholey, J. M. & Vale, R. D. Length control of the metaphase spindle. *Curr. Biol.* **15**, 1979–1988 (2005).
- Pereira, A. J., Dalby, B., Stewart, R. J., Doherty, S. J. & Goldstein, L. S. Mitochondrial association of a plus end-directed microtubule motor expressed during mitosis in *Drosophila*. *J. Cell Biol.* **136**, 1081–1090 (1997).
- Rischitor, P. E., Konzack, S. & Fischer, R. The Kip3-like kinesin KipB moves along microtubules and determines spindle position during synchronized mitoses in *Aspergillus nidulans* hyphae. *Eukaryot. Cell* **3**, 632–645 (2004).
- Tytell, J. D. & Sorger, P. K. Analysis of kinesin motor function at budding yeast kinetochores. *J. Cell Biol.* **172**, 861–874 (2006).
- Zhu, C. *et al.* Functional analysis of human microtubule-based motor proteins, the kinesins and dyneins, in mitosis/cytokinesis using RNA interference. *Mol. Biol. Cell* **16**, 3187–3199 (2005).

20. Miki, H., Okada, Y. & Hirokawa, N. Analysis of the kinesin superfamily: insights into structure and function. *Trends Cell Biol.* **15**, 467–476 (2005).
21. Severin, F., Habermann, B., Huffaker, T. & Hyman, T. Stu2 promotes mitotic spindle elongation in anaphase. *J. Cell Biol.* **153**, 435–442 (2001).
22. Ogawa, T., Nitta, R., Okada, Y. & Hirokawa, N. A common mechanism for microtubule destabilizers—M type kinesins stabilize curling of the protofilament using the class-specific neck and loops. *Cell* **116**, 591–602 (2004).
23. Shipley, K. *et al.* Structure of a kinesin microtubule depolymerization machine. *EMBO J.* **23**, 1422–1432 (2004).
24. Cottingham, F. R., Gheber, L., Miller, D. L. & Hoyt, M. A. Novel roles for *Saccharomyces cerevisiae* mitotic spindle motors. *J. Cell Biol.* **147**, 335–350 (1999).
25. Straight, A. F., Sedat, J. W. & Murray, A. W. Time-lapse microscopy reveals unique roles for kinesins during anaphase in budding yeast. *J. Cell Biol.* **143**, 687–694 (1998).
26. Waterman-Storer, C. M., Desai, A., Bulinski, J. C. & Salmon, E. D. Fluorescent speckle microscopy, a method to visualize the dynamics of protein assemblies in living cells. *Curr. Biol.* **8**, 1227–1230 (1998).
27. Akhmanova, A. & Hoogenraad, C. C. Microtubule plus-end-tracking proteins: mechanisms and functions. *Curr. Opin. Cell Biol.* **17**, 47–54 (2005).
28. Howard, J. & Hyman, A. A. Preparation of marked microtubules for the assay of the polarity of microtubule-based motors by fluorescence microscopy. *Methods Cell Biol.* **39**, 105–113 (1993).
29. Hyman, A. A., Salsler, S., Drechsel, D. N., Unwin, N. & Mitchison, T. J. Role of GTP hydrolysis in microtubule dynamics: information from a slowly hydrolyzable analogue, GMPCPP. *Mol. Biol. Cell* **3**, 1155–1167 (1992).
30. Desai, A., Verma, S., Mitchison, T. J. & Walczak, C. E. Kin I kinesins are microtubule-destabilizing enzymes. *Cell* **96**, 69–78 (1999).
31. Hunter, A. W. *et al.* The kinesin-related protein MCAK is a microtubule depolymerase that forms an ATP-hydrolyzing complex at microtubule ends. *Mol. Cell* **11**, 445–457 (2003).
32. Liakopoulos, D., Kusch, J., Grava, S., Vogel, J. & Barral, Y. Asymmetric loading of Kar9 onto spindle poles and microtubules ensures proper spindle alignment. *Cell* **112**, 561–574 (2003).
33. Pearson, C. G. & Bloom, K. Dynamic microtubules lead the way for spindle positioning. *Nature Rev. Mol. Cell Biol.* **5**, 481–492 (2004).
34. Adames, N. R. & Cooper, J. A. Microtubule interactions with the cell cortex causing nuclear movements in *Saccharomyces cerevisiae*. *J. Cell Biol.* **149**, 863–874 (2000).
35. Maddox, P. S., Stemple, J. K., Satterwhite, L., Salmon, E. D. & Bloom, K. The minus end-directed motor Kar3 is required for coupling dynamic microtubule plus ends to the cortical shmoo tip in budding yeast. *Curr. Biol.* **13**, 1423–1428 (2003).
36. Brunner, D. & Nurse, P. CLIP170-like tip1p spatially organizes microtubular dynamics in fission yeast. *Cell* **102**, 695–704 (2000).
37. Tran, P. T., Marsh, L., Doye, V., Inoue, S. & Chang, F. A mechanism for nuclear positioning in fission yeast based on microtubule pushing. *J. Cell Biol.* **153**, 397–411 (2001).
38. Komarova, Y. A., Vorobjev, I. A. & Borisy, G. G. Life cycle of MTs: persistent growth in the cell interior, asymmetric transition frequencies and effects of the cell boundary. *J. Cell Sci.* **115**, 3527–3539 (2002).
39. Bringmann, H. *et al.* A kinesin-like motor inhibits microtubule dynamic instability. *Science* **303**, 1519–1522 (2004).
40. Mennella, V. *et al.* Functionally distinct kinesin-13 family members cooperate to regulate microtubule dynamics during interphase. *Nature Cell Biol.* **7**, 235–245 (2005).
41. Moore, A. T. *et al.* MCAK associates with the tips of polymerizing microtubules. *J. Cell Biol.* **169**, 391–397 (2005).
42. Wadsworth, P. Regional regulation of microtubule dynamics in polarized, motile cells. *Cell Motil. Cytoskeleton* **42**, 48–59 (1999).
43. Wittmann, T., Bokoch, G. M. & Waterman-Storer, C. M. Regulation of leading edge microtubule and actin dynamics downstream of Rac1. *J. Cell Biol.* **161**, 845–851 (2003).
44. Labbe, J. C., Maddox, P. S., Salmon, E. D. & Goldstein, B. PAR proteins regulate microtubule dynamics at the cell cortex in *C. elegans*. *Curr. Biol.* **13**, 707–714 (2003).
45. Kline-Smith, S. L. & Walczak, C. E. The microtubule-destabilizing kinesin XKCM1 regulates microtubule dynamic instability in cells. *Mol. Biol. Cell* **13**, 2718–2731 (2002).
46. Rose, M. D., Winston, F. & Hieter, P. *Methods in Yeast Genetics* (Cold Spring Harbor Laboratory Press, 1990).
47. Hyman, A. *et al.* Preparation of modified tubulins. *Methods Enzymol.* **196**, 478–485 (1991).
48. Paschal, B. M. & Vallee, R. B. Microtubule and axoneme gliding assays for force production by microtubule motor proteins. *Methods Cell Biol.* **39**, 65–74 (1993).
49. Huang, T. G. & Hackney, D. D. *Drosophila* kinesin minimal motor domain expressed in *Escherichia coli*. Purification and kinetic characterization. *J. Biol. Chem.* **269**, 16493–16501 (1994).
50. Tirmauer, J. S., O'Toole, E., Berrueta, L., Bierer, B. E. & Pellman, D. Yeast Bim1p promotes the G1-specific dynamics of microtubules. *J. Cell Biol.* **145**, 993–1007 (1999).

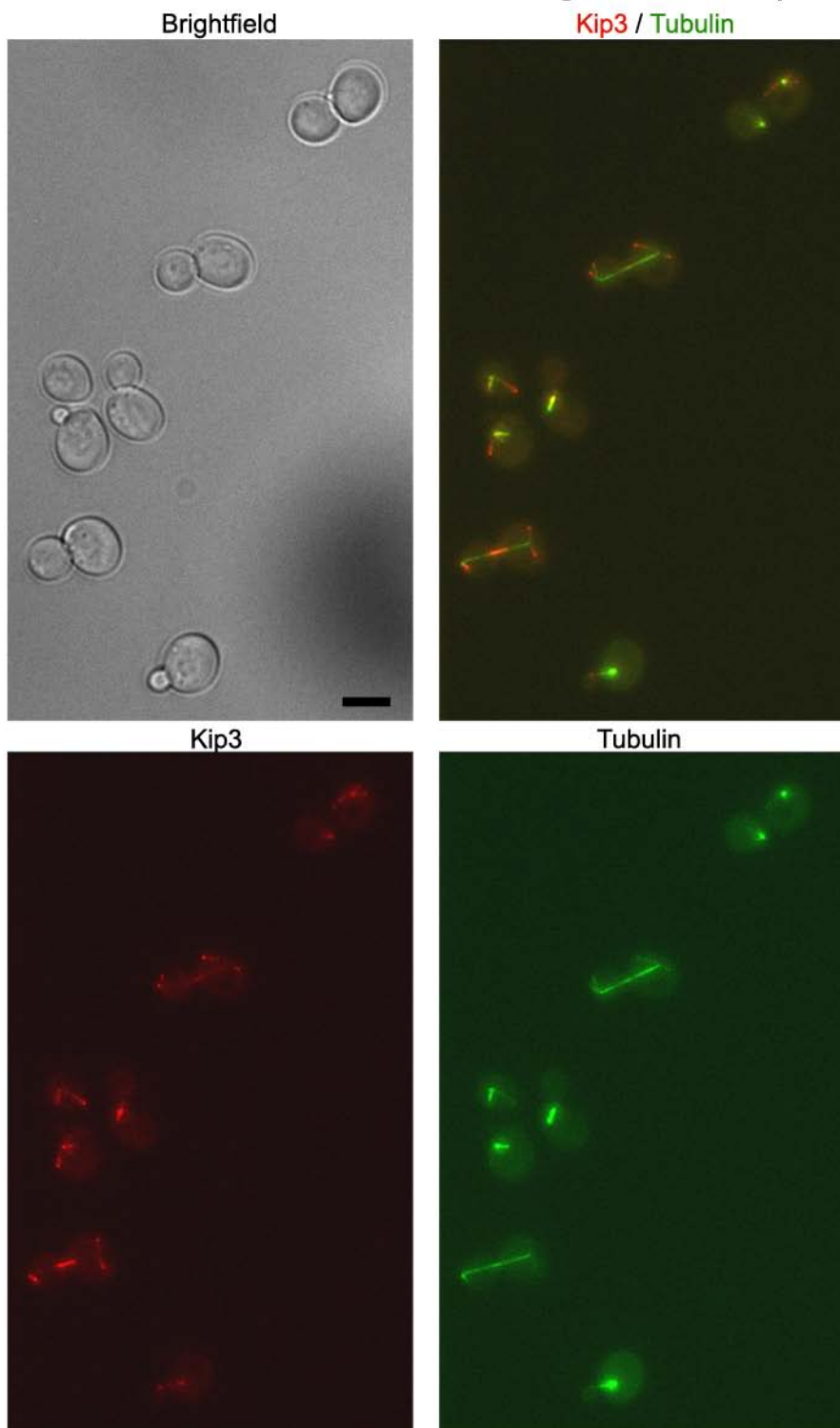


**Figure S1. Localization of Kip3p-3YFP (red in merged image) and CFP-Tub1p (green in merged image).** The panels show two-dimensional projection images of three-dimensional z-series images. This figure shows a field of cells rather than the images of single cells presented in Figure 1. Bar = 5  $\mu$ m.

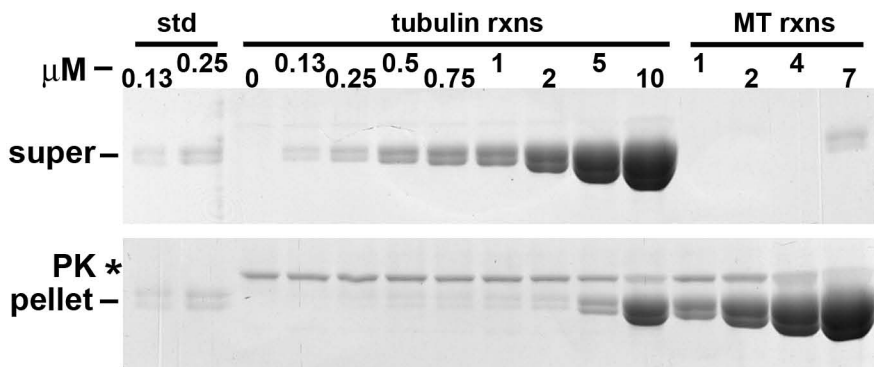


**Figure S2. The tubulin-activated ATPase of Kip3p cannot be attributed to microtubules in the ATPase reactions.** Control sedimentation analysis for microtubule assembly in parallel samples to the tubulin-activated ATPase reactions in Figure 4a. Identical reactions (100  $\mu$ l) were prepared immediately following the ATPase assay and with the same reagents. After incubation the reactions were centrifuged at 250,000  $\times$  g for 20 min (25°C). The supernatants were gently removed and the pellets were resuspended (without rinsing) in 100  $\mu$ l of BRB80. Equal volumes of supernatant (super) and pellet were analyzed by Coomassie-stained SDS-PAGE. Lanes marked 'tubulin rxns' contained soluble tubulin dimers and Kip3p. Lanes marked 'MT rxns' contained Taxol-stabilized polymeric tubulin for comparison of sedimentation, but lacked Kip3p. Lanes marked 'std' were loaded with a tubulin concentration identical to the total (super + pellet) tubulin concentration in the equivalent soluble tubulin reactions. For each lane,  $\mu$ M indicates the concentration of tubulin in the reaction. The increase in Kip3p tubulin-activated ATPase is most dramatic from 0 to 1  $\mu$ M tubulin, a range we did not detect a corresponding increase in polymeric tubulin (pellet). Note: we detected 0.13  $\mu$ M tubulin in both control lanes, as well as in the supernatant of the corresponding tubulin reaction. Thus, any contaminating polymer must remain below this level. The increased tubulin in the pellet fraction between 2 and 10  $\mu$ M is likely to be carryover from the high supernatant concentration since the tubes were not rinsed after aspiration. Alternatively, it may represent aggregated tubulin. Regardless, Kip3p tubulin-activated ATPase was already nearly saturated with 2  $\mu$ M of this tubulin solution. The band marked by an asterisk (\*) corresponds to the MW of pyruvate kinase (57 kDa) that was added in equal amounts to all reactions. Additionally, the activation of Kip3p ATPase activity by tubulin saturated with a maximum rate that was only ~25% of that achieved with microtubules, before the half-maximal concentration for microtubule-activated ATPase was reached. If the stimulatory effect was due to contaminating polymer, additional amounts of this polymer should continue to increase the Kip3p ATPase activity up to what we measured as the polymer-activated maximum. For the same reasons we can also conclude that Kip3p did not promote the nucleation of microtubules *de novo* under the reaction conditions used.

## Salt dependence of Kip3 tubulin-activated ATPase activity

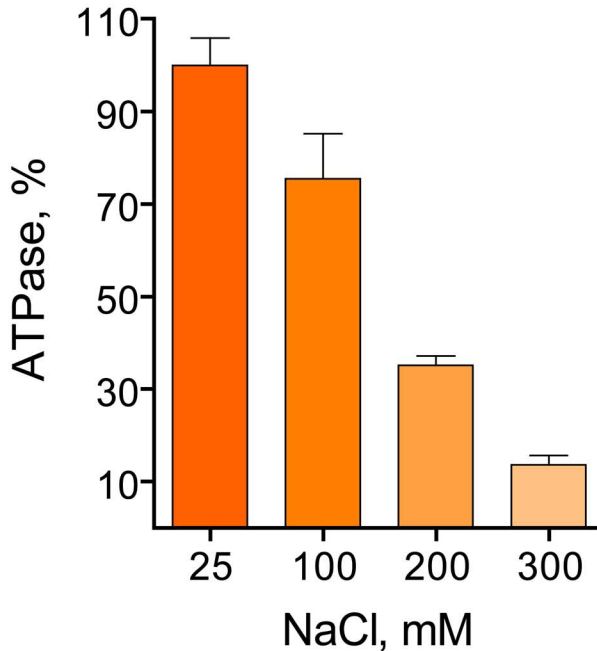


**Figure S3. Kip3p tubulin-activated ATPase is inhibited by high salt concentration.** Steady-state ATPase reactions containing 200 nM Kip3p and 3  $\mu$ M tubulin dimer were conducted as in Figure 4a. The ATPase rates (mean  $\pm$  SEM) are graphed as the percentage of ATPase activity measured in 25 mM salt. Control reactions verified that the enzyme-linked NADH oxidation reaction did not become rate-limiting at any salt concentration.

**Protein Expression and Purification**

For the purification of Kip3p expressed by baculovirus in insect cells:  $2.5 \times 10^8$  Kip3p-expressing Hi5 cells from 250 ml of culture were resuspended and homogenized with a loose-fitting Potter-Elvehjem homogenizer in 30 ml ice-cold insect lysis buffer [50 mM NaPO<sub>4</sub>, 500 mM NaCl, 10% glycerol, 1% Triton X-100, 40 mM imidazole, 3 mM DTT, 0.5 mM ATP, 1 mM PMSF, and Complete protease inhibitor mix (Roche Diagnostics), pH 7.5]. All subsequent steps were performed on ice or at 4°C. The lysate was cleared for 30 min at 100,000×g and then combined with 1.3 ml Ni-Sepharose (Amersham Biosciences) pre-equilibrated in lysis buffer. After tumbling 20 min, the resin was washed three times by 5 min tumbling with 15 ml insect lysis buffer (adjusted to 25 mM imidazole, 0.5 mM DTT, 0.1 mM ATP, and without Triton X-100). The washed resin was packed into a 5 mm I.D. column with a minimal amount of wash buffer and eluted using insect lysis buffer (adjusted to 25 mM NaPO<sub>4</sub>, 300 mM NaCl, 350 mM imidazole, 0.5 mM DTT, 0.1 mM ATP, 0.5 mM PMSF, and without Triton X-100). Peak protein-containing fractions (0.5 ml) were pooled and cleared at 100,000×g for 15 min. The protein mixture was next adjusted to 250 mM NaCl and applied to a BioRad Uno S ion exchange column (6 ml bed, equilibrated in 50 mM HEPES, 250 mM NaCl, pH 7.5). The column was developed with a linear gradient to 1 M NaCl over 12 column volumes. The majority of protein eluted as a single peak ( $A_{280}$ ) around 500 mM NaCl. The major protein fractions were pooled, spiked with 50 μM ATP, concentrated using a microcon YM-50 (Millipore), and then dialyzed against 25 mM HEPES, 300 mM NaCl, 100 μM

ATP, and 10% sucrose, pH 7.5. Finally, the protein was centrifuged at 150,000×g for 10 min, snap-frozen in liquid N<sub>2</sub> and stored at –80°C.

To obtain Kip3p from yeast cells, expression from pB2537 was induced for 12 h at 30°C. The cells were then washed in ice-cold water and drop frozen into liquid N<sub>2</sub> as a slurry in 1/3 volume of the same. The frozen cell pellets were lysed by mechanical disruption<sup>1</sup> using an electric coffee grinder and the powder was kept frozen and stored at –80°C. For purification 10 g of yeast cell powder was thawed and immediately resuspended into 20 ml of ice-cold yeast lysis buffer [50 mM NaPO<sub>4</sub>, 300 mM NaCl, 1% NP-40, 30 mM imidazole, 0.5 mM DTT, 0.5 mM ATP, 2 mM PMSF, and Complete protease inhibitor mix (Roche Diagnostics), pH 7.6]. All subsequent steps were performed on ice or at 4°C. The lysate was sonicated for 30 s before clearing with a 45 min spin at 100,000×g. Next, the cleared lysate was applied batch-wise to 0.5 ml Ni-NTA (Qiagen) for 2 h with tumbling. The resin was then washed 2 × 10 ml (10 min) with 25 mM NaPO<sub>4</sub>, 500 mM NaCl, 20 mM imidazole, 0.5 mM DTT, 0.1 mM ATP, and 5% glycerol, pH 7.6. The washed Ni-NTA was loaded into a 5 mm I.D. column and eluted with wash buffer containing 350 mM imidazole, pH 8. The protein-containing fractions from the Ni-NTA column were pooled and bound batch-wise for 1 h to 2 ml of Strep-Tactin resin (Qiagen). This resin was next washed with 2 × 10 ml Ni-NTA elution buffer without imidazole, loaded into a column with the same, and eluted with 50 mM NaPO<sub>4</sub>, 300 mM NaCl, 0.1 mM ATP, and 2.5 mM desthiobiotin, pH 8. The 2 ml eluate following the void volume was collected and a microcon YM-50 was used to concentrate and exchange the buffer to 25 mM NaPO<sub>4</sub>, 300 mM NaCl, and 10% sucrose, pH 7.5. The

protein was stored as above. Protein concentrations were determined by the Bradford method<sup>2</sup>. Concentrations reported refer to monomeric Kip3p.

### **Preparation of Tubulin and Stabilized Microtubules**

Bovine brain tubulin was purified by successive rounds of temperature-dependent polymerization<sup>3</sup> followed by phosphocellulose chromatography<sup>4</sup>. Bright (1:4) rhodamine- or dim (1:10) fluorescein-labeled seeds were polymerized using ~20  $\mu\text{M}$  tubulin and 0.5 mM GMPCPP in BRB80 (80 mM potassium PIPES, 1 mM EGTA, 1 mM  $\text{MgCl}_2$ , pH 6.9). Dim (1:20) rhodamine-labeled elongation of the seeds was achieved by diluting the seeds ~1:50 into 1.5-2  $\mu\text{M}$  tubulin with 0.5 mM GMPCPP during warming and incubating for 2 h at 37°C. To inhibit minus end elongation, the polarity marked elongation mix contained 2  $\mu\text{M}$  dim rhodamine-tubulin and 1.6  $\mu\text{M}$  NEM-tubulin<sup>5</sup>. After preparation, the GMPCPP-stabilized microtubules were pelleted, resuspended in BRB80, and kept at room temperature. For paclitaxel (Taxol)-stabilized microtubules the purified tubulin was thawed and cleared by ultracentrifugation prior to assembly in BRB80 plus 0.5 mM GTP and 8% DMSO for 30 min at 37°C followed by the incremental addition of Taxol (2 mM in DMSO) to 20  $\mu\text{M}$ . The stabilized microtubules were then pelleted, resuspended in BRB80 plus 10  $\mu\text{M}$  Taxol, and kept at room temperature. The concentration of tubulin in the stabilized microtubule suspensions was determined by the Bradford method or by  $A_{280}$  ( $\epsilon=115,000 \text{ M}^{-1}\text{cm}^{-1}$ ) after  $\text{Ca}^{++}$  and cold depolymerization.

AMPPNP, N-ethylmaleimide, and Taxol were purchased from Sigma. GMPCPP was obtained from Jena Bioscience. Fluorescein-, rhodamine-, and biotin-tubulin was purchased from Cytoskeleton.

## Motility and Depolymerase Assays

Microtubule gliding assays were conducted using the basic techniques described by Paschal and Vallee<sup>6</sup>. Acid-washed perfusion chambers were blocked with 2.5 mg/ml casein in BRB80, followed by addition of ~50 µg/ml Kip3p (in BRB80, 0.2 mg/ml casein, 0.1 mM ATP + 30 mM KCl). After 5 min, the chamber was washed with 4 volumes of the same buffer without Kip3p. Subsequently, 1.5 volumes of stabilized microtubules in BRB80 + 0.2 mg/ml casein + 2 mM ATP + 75 mM KCl was exchanged into the flowcell and fluorescent images recorded every 30-60 s. Washing and reaction mixtures contained oxygen scavenging mix (OSM; 200 µg/ml glucose oxidase, 35 µg/ml catalase, 25 mM glucose, and 70 mM βME). Microtubule velocities were determined for continuous movement over at least 4 timepoints (>2-4 min) using the red/green interface on the microtubule as a reference. For AMPPNP, 2 mM analogue was included in the microtubule mix and ATP was omitted from washing and reaction solutions. The control kinesin heavy chain fragments (GST-KHC<sup>1-379</sup> and KHC<sup>1-560</sup>-His<sub>6</sub>) were adhered to flowcells prior to blocking.

To determine microtubule depolymerization rates, bright/dim segmented, GMPCPP-stabilized microtubules were polymerized with a 1:200 molar ratio of biotin-modified tubulin. Flowcells were coated with anti-biotin antibody, blocked, and then washed with 5 volumes BRB80 + 0.2 mg/ml casein. Reactions contained BRB80 + 0.2 mg/ml casein, 0.5 mM DTT, 25 mM KCl, 2 mM ATP/AMPPNP, OSM, and microtubules. Kip3p or control proteins were added last, 1.5 volumes perfused into the chamber, and images recorded every 30 s. Microtubules were scored for polarity if the

plus end segment was at least twice as long as the minus end segment. Using this criteria ~90% of the microtubules depolymerized exclusively on the longer end, while the remaining ~10% depolymerized exclusively on the shorter segment with similar rates. Microtubule lengths were measured with respect to the bright/dim interface.

#### **SUPPLEMENTARY REFERENCES**

1. Sorger, P. K. & Pelham, H. R. Purification and characterization of a heat-shock element binding protein from yeast. *Embo J.* **6**, 3035-41 (1987).
2. Bradford, M. M. A rapid and sensitive method for the quantitation of microgram quantities of protein utilizing the principle of protein-dye binding. *Anal. Biochem.* **72**, 248-54 (1976).
3. Algaier, J. & Himes, R. H. The effects of dimethyl sulfoxide on the kinetics of tubulin assembly. *Biochim. Biophys. Acta.* **954**, 235-43 (1988).
4. Tiwari, S. C. & Suprenant, K. A. A pH- and temperature-dependent cycling method that doubles the yield of microtubule protein. *Anal. Biochem.* **215**, 96-103 (1993).
5. Hyman, A. et al. Preparation of modified tubulins. *Methods Enzymol.* **196**, 478-85 (1991).
6. Paschal, B. M. & Vallee, R. B. Microtubule and axoneme gliding assays for force production by microtubule motor proteins. *Methods Cell Biol.* **39**, 65-74 (1993).

**Supplementary Video SV1. Kip3p translocates towards microtubule plus ends in vivo.** Imaging of Kip3p-3YFP (red) and CFP-Tubulin (green) in an anaphase cell. Kip3p ‘speckles’ are marked by arrowheads. Elapsed time between frames is 2.5 s and the entire timelapse lasts 240 s.

**Supplementary Video SV2. Kip3p is lost from the plus ends of shrinking microtubules.** Imaging of Kip3p-3YFP (red) and CFP-Tubulin (green) in a G1 cell. The microtubule plus end is marked by the arrow. Elapsed time between frames is 5.5 s and the entire timelapse lasts 105 s.

**Supplementary Video SV3. Kip3p is a plus end-directed motor (insect cell-derived).** Microtubule gliding assay using Kip3p purified from insect cells. Minus ends are green and plus ends are red. Plus end-specific depolymerization is also apparent in this experiment.

**Supplementary Video SV4. Kip3p is a plus end-directed motor (yeast-derived).** Microtubule gliding assay using Kip3p purified from yeast cells. Minus ends are green and plus ends are red. Plus end-specific depolymerization is also apparent in this experiment.

**Supplementary Video SV5. Plus end-specific depolymerase activity of Kip3p (insect cell-derived).** 100 nM polymerized tubulin (bright/dim GMPCPP-stabilized microtubules) was combined with 10 nM Kip3p plus ATP. The microtubules were anchored to the coverslip via biotin-modified tubulin (1:200). The majority of plus ends can be identified as the longer dim segment.

**Supplementary Video SV6. Plus end-specific depolymerase activity of Kip3p (yeast-derived).** 100 nM polymerized tubulin (bright/dim GMPCPP-stabilized microtubules) was combined with 25 nM Kip3p plus ATP. The microtubules were anchored to the coverslip via biotin-modified tubulin (1:200). The majority of plus ends can be identified as the longer dim segment.

**Supplementary Video SV7. Plus end-specific depolymerase activity of Kip3p (high concentration, insect cell-derived).** 100 nM polymerized tubulin (bright/dim GMPCPP-stabilized microtubules) was combined with 50 nM Kip3p plus ATP. The microtubules were anchored to the coverslip via biotin-modified tubulin (1:200). The majority of plus ends can be identified as the longer dim segment.

**Supplementary Video SV8. *Xenopus* MCAK depolymerizes both ends of microtubules.** 100 nM polymerized tubulin (bright/dim GMPCPP-stabilized microtubules) was combined with 10 nM MCAK plus ATP. The microtubules were anchored to the coverslip via biotin-modified tubulin (1:200).

**Supplementary Video SV9. Microtubules in *kip3* $\Delta$  cells continue to grow after contacting the bud cortex (arrow).** Microtubules are visualized with GFP-Tubulin. Time elapsed between frames is 8 s. Entire timelapse represents 520 s.

**Supplementary Video SV10. Microtubules in wild-type cells briefly pause and do not grow during contact with the bud cortex.** Microtubules are visualized with GFP-Tubulin. Time elapsed between frames is 8 s. Entire timelapse represents 256 s.